Influence of Polydispersity on the Self-Assembly of Diblock Copolymers

Nathaniel A. Lynd and Marc A. Hillmyer*

Department of Chemistry, University of Minnesota, 207 Pleasant St. SE, Minneapolis, Minnesota 55455-0431

Received May 18, 2005; Revised Manuscript Received July 25, 2005

ABSTRACT: The domain sizes and morphological boundaries in diblock copolymers have been predicted to be influenced by changes in the molecular weight distribution of one or both of the blocks. To systematically explore these effects, we prepared several sets of poly(ethylene-*alt*-propylene)-*b*-poly(DL-lactide) diblock copolymers with controlled molecular weights, compositions, and polydispersity indices. The polydispersity of the polylactide block was controlled by taking advantage of the equilibrium nature of the ring-opening polymerization of lactide. Small-angle X-ray scattering was used to evaluate the influence of block copolymer polydispersity on the equilibrium domain spacing and resultant ordered state morphology. We found that the domain spacing increased with increasing polydispersity and demonstrated that an increase in polydispersity at constant polylactide composition can result in a change in morphology for compositionally asymmetric diblock copolymers. More specifically, when the polylactide block is the minority component, a polydispersity increase in that block results in a change of morphology to one with larger mean interfacial curvature. Conversely, an increase in the polydispersity of the polylactide segment in a block copolymer with a majority of polylactide drives transitions to structures with smaller mean interfacial curvature. The experimental results were corroborated by self-consistent mean-field theory.

Introduction

Thermodynamic incompatibility between two covalently end connected polymers in AB diblock copolymers results in microphase separation of the distinct segments into ordered structures with compositional heterogeneities on a nanometer length scale.[1] The energetic interplay between interfacial segment−segment contact and chain stretching dictates the principal domain spacing and ordered state symmetry adopted by the material. The four equilibrium structures that have been observed in several AB diblock copolymer systems and supported by self-consistent mean-field theory are a lamellar structure (L), hexagonally packed cylinders (C), a complex bicontinuous structure called gyroid (G), and body-centered-cubic spheres (S). The specific morphology adopted by an ordered AB diblock copolymer system depends on the composition of the diblock copolymer, f_A, the volume fraction of the A component in an AB diblock copolymer ($f_B = 1 - f_A$), and the degree of segregation between the A and B segments, which is the product of the total number-average of segments (N) and the effective interaction parameter per segment, χ.

All synthetic methods of producing macromolecules result in a distribution of segment sizes, and the polydispersity index (PDI = M_w/M_n) characterizes the breadth of this molecular weight distribution (MWD). For block copolymers, an increase in PDI results in a distribution in both chain length (N) and composition (f_A). In light of this fact, in 1980 Leibler intimated the importance of studying the effects of an increased PDI on both order−disorder and order−order transitions of block copolymers.[2] Since then, mean-field theoretical treatments aimed at explaining the influence of the MWD on block copolymers at various degrees of segregation have appeared in the literature. Leibler and Benoit[3] in 1981 and Hong and Noolandi[4] in 1984 were the first to include the effects of increased PDI into the framework of the random phase approximation (RPA) for disordered block copolymer melts using continuous Schultz−Zimm distributions to model the MWD of block copolymers. Both publications noted that the spatial frequency of the dominant composition fluctuation, q^*, decreased as PDI increased. This is due to the presence of larger chains in the melt as PDI is increased. The other notable effect was increased disordered state scattered intensity at q^* as PDI was increased, indicating that as the MWD became broader, the system neared its spinodal, corresponding to the order−disorder transition (ODT) in these studies. These results lead one to expect that a system with increased PDI will both order more readily and possess greater domain spacing than its monodisperse counterpart at equivalent number-average molecular weight and composition.

In 1989, Milner, Witten, and Cates investigated polymer brushes, a system that is analogous to ordered diblock copolymers, using strong segregation theory for a strongly segregated polymer brush.[5] They found that a polydisperse brush was much taller than its monodisperse analogue due to the greater ability of the larger chains to fill space at the outward edge of the brush. In addition, the mixing of chains with different lengths was energetically favored due to an increase of the brush configurational entropy (i.e., increasing PDI reduces the stretching energy of a polymer brush).

In related work, Burger, Ruland, and Semenov[6,7] extended the weak segregation theory (WST) pioneered by Leibler[2] and Fredrickson and Helfand[8] and explained the influence of the MWD on the disordered state scattering and ordered phase behavior. They predicted that the degree of segregation at the ODT, $(\chi N)_{ODT}$, decreases significantly upon a symmetrical increase in PDI of both blocks at all compositions. Also, the regions of stability for the various morphologies shifted and increased in area significantly upon PDI increase. Specifically, the lamellar region of the phase diagram

* To whom correspondence should be addressed. E-mail: hillmyer@chem.umn.edu.

10.1021/ma051025r CCC: $30.25
Published on Web 09/10/2005

at a PDI of 1 and $\chi N = 14$ spans from $f = 0.38$ to $f = 0.62$, whereas at a PDI of 2 this region extends from $f = 0.27$ to $f = 0.73$.

Recently, Sides and Fredrickson developed an efficient method of using self-consistent mean-field theory (SCMFT) to investigate the effects of increasing the PDI of one block while setting the PDI of the other block to 1.[9] Two-dimensional simulations of the cylindrical morphology also indicated that a PDI increase enlarged the equilibrium unit cell (i.e., increased the domain spacing) and exhibited a partitioning by chain lengths within the unit cell; the larger chains fill the centers of the domains whereas the shorter chains remain localized near the interface. Using three-dimensional simulations, they demonstrated a change in morphology from C to S at fixed average composition ($f = 0.30$) and segregation ($\chi N = 18.0$) upon an increase in the PDI of the minority block from 1.0 to 1.5. When both blocks are monodisperse in a more symmetrical system ($f = 0.45$), a lamellar morphology results. As the PDI of the minority component was increased to 1.5, a complex bicontinuous morphology resulted, followed by a transition to a pseudohexagonally packed cylinder morphology upon a further PDI increase to 1.67 of the minority component. Although the latter two morphologies were not fully equilibrated, these calculations effectively demonstrate the dramatic influence of the MWD on the ordered phase behavior of diblock copolymers. At no point was macrophase separation observed when PDI was increased using continuous distributions.

A few experimental studies on the effects of MWD on diblock copolymer self-assembly have appeared in the literature. Matsushita et al. synthesized a series of polystyrene-*b*-poly(2-vinylpyridine) (PS−PVP) diblock copolymers with narrow MWDs (PDI ≤ 1.06) and a range of compositions ($0.1 < f_{PS} < 0.9$) at molecular weights between 100 and 160 kg mol^{-1}.[10] Blends were prepared with different degrees of compositional polydispersity about an average composition of $f = 0.5$. These blends were characterized by the PDI of the PS block (1.03−1.85) but with M_n between 128 and 136 kg mol^{-1}. They observed that as the PDI of the PS block increased, the lamellar domain spacing increased until the PDI of the PS block reached 1.8. Above PDI = 1.8 macrophase separation occurred. In addition to this work, Bendejaq et al. synthesized several polystyrene-*b*-poly(acrylic acid) diblock copolymers with broad MWDs and found that these systems produced well-ordered structures.[11] No macrophase separation occurred for the case of neat polydisperse diblock copolymers, although C and L coexistence was observed for homopolymer/diblock copolymer blends.

Given that many contemporary synthetic protocols for the synthesis of diblock copolymers yield materials with relatively broad molecular weight distributions (relative to, for example, living anionic polymerization) and the theoretical work that has established the importance of MWD on the self-assembly of diblock copolymers, we designed an experimental system aimed at systematically uncovering the influence of PDI on block copolymer self-assembly. For this we chose a set of poly(ethylene-*alt*-propylene)-*b*-poly(DL-lactide) (PEP−PLA) diblock copolymers. These are particularly well suited to explore the effects of increased PDI on ordered block copolymer melts due to the ease of synthesis of controlled-PDI materials. Anionic polymerization of isoprene and selective end capping with ethylene oxide followed by catalytic hydrogenation affords a hydroxy-terminated PEP block with a very narrow MWD. Polylactide can be grown from this PEP block, and the equilibrium nature of the lactide polymerization allows the PDI of the PLA block to be independently increased while keeping the overall average composition and M_n fixed. No blending is required, and the effects of an increase in the breadth of the MWD of one block may easily be investigated. In addition, the phase behavior of the conformationally symmetric PEP−PLA system has been previously established.[12,13] By preparing several sets of PEP−PLA block copolymers at different compositions and PDIs, we were able to systematically explore the effects of increased PDI on domain spacing and morphological transitions in these materials.

Experimental Section

Materials. All materials were used as received unless otherwise indicated. Isoprene (Aldrich) was distilled twice from *n*-butyllithium (Aldrich, 2.5 M in hexanes) at 0 °C under reduced pressure. Ethylene oxide (Aldrich) was stirred over CaH_2 (Aldrich) at 0 °C overnight and dibutylmagnesium (Aldrich, 1.0 M in heptane) for 4 h before vacuum distillation. DL-Lactide (Aldrich) was recrystallized from ethyl acetate, dried in vacuo at RT overnight, and stored under a nitrogen atmosphere. Toluene and cyclohexane were both purified by passing through an activated alumina (LaRoche) column to remove protic impurities and a supported copper catalyst (Q-5 Engehardt) to remove trace amounts of oxygen.[14]

Molecular Characterization. Molecular weights of hydroxy-terminated PEP (PEP−OH) and PEP−PLA and conversion of lactide were determined by ^{1}H NMR spectroscopy at 500 MHz using a Varian Inova 500 spectrometer. Samples were dissolved in $CDCl_3$ (Cambridge Isotope Laboratories) at concentrations of about 1.0 wt %. 16 scans were taken per spectrum with a delay time of 20 s between consecutive pulses. PDI was determined using size exclusion chromatography (SEC) on a Hewlett-Packard 1100 series liquid chromatograph fitted with a Hewlett-Packard 1047A refractive index detector and three Jordi polydivinylbenzene columns with 10^4, 10^3, and 500 Å pore sizes and calibrated with polystyrene standards (Polymer Laboratories). Tetrahydrofuran was used as the mobile phase with a flow rate of 1 mL/min at 40 °C. To determine the precision of the PDI measurement, 20 solutions of a single PEP−PLA (Table 1, PL(0.50,1.94)-1) were prepared independently and run consecutively. The PDIs of all samples agreed to within ±0.01.

Synthesis of Poly(ethylene-*alt*-propylene)-*b*-poly(DL-lactide) (PEP−PLA). The synthesis of hydroxyl-terminated poly(4,1-isoprene) (PI−OH), and subsequent catalytic hydrogenation to PEP−OH has been reported previously.[12] The macroinitiator for the polymerization of lactide was formed from the reaction of triethylaluminum with PEP−OH in toluene at $[Al]_0/[PEP-OH]_0 = 0.5$.[12,15] DL-Lactide (LA) was added at room temperature such that $[LA]_0 = 1.0$ M, and the reaction was stirred at 90 °C. A typical procedure is as follows: a 48 mL Chemglass high-pressure vessel equipped with an internal thread was treated with a 90:10 solution (by volume) of methylene chloride/dichlorodimethylsilane and allowed to dry at 70 °C overnight. The silanized vessel, a magenetic Teflon-coated stir bar, and typical PEP−OH (0.5 g) were transferred to a glovebox (N_2 environment). The PEP−OH was dissolved in toluene. Triethylaluminum (0.5 equiv to PEP−OH) was added to the solution via syringe and allowed to stir for at least 4 h at room temperature. LA was then added to the flask such that the concentration of LA was 1.0 M. The vessel was then sealed with a Teflon bushing and a Viton O-ring and removed from the glovebox. The reaction vessel was immersed in an oil bath at 90 °C and allowed to stir until the equilibrium conversion was reached. Reactions were terminated with 1.5 M HCl followed by precipitation in methanol. Polymers were isolated by filtration, rinsed with

Table 1. Molecular and Morphological Characteristics of Diblock Copolymers

sample ID	N_{total}[a]	f_{PLA}[a]	PDI[b]	PDI_{PLA}[b]	M_n^{PLA} (kg/mol)[c]	M_n (kg/mol)[c]	phase[d]	D[e]
PL(0.51,1.42)-1	148	0.507	1.16	1.42	9.17	15.2	L	28.9
PL(0.51,1.56)-1	148	0.507	1.21	1.56	9.17	15.2	L	29.6
PL(0.49,1.71)-1	144	0.491	1.25	1.71	8.61	14.7	L	29.6
PL(0.51,1.82)-1	149	0.509	1.31	1.82	9.22	15.3	L	31.6
PL(0.51,1.89)-1	150	0.512	1.33	1.89	9.34	15.4	L	32.1
PL(0.50,1.94)-1	145	0.498	1.34	1.94	8.84	14.9	L	31.9
PL(0.49,1.36)-2	25.9	0.494	1.15	1.36	1.56	2.64	L	9.73
PL(0.48,1.35)-2	25.1	0.478	1.14	1.35	1.47	2.55	L	9.73
PL(0.47,1.45)-2	24.8	0.472	1.17	1.45	1.42	2.50	L	9.52
PL(0.49,1.49)-2	25.5	0.486	1.19	1.49	1.52	2.60	L	9.94
PL(0.47,1.61)-2	24.6	0.467	1.22	1.61	1.40	2.48	L	9.73
PL(0.46,1.82)-2	24.2	0.459	1.28	1.82	1.35	2.43	L	9.94
PL(0.46,1.82)-2	24.2	0.459	1.28	1.82	1.36	2.44	L	9.62
PL(0.50,1.22)-3	28.5	0.541	1.11	1.22	1.88	2.96	L	10.6
PL(0.51,1.32)-3	29.1	0.551	1.15	1.32	1.96	3.04	L	11.0
PL(0.51,1.35)-3	28.8	0.547	1.16	1.35	1.93	3.01	L	10.7
PL(0.51,1.45)-3	29.3	0.554	1.20	1.45	1.98	3.06	L	11.7
PL(0.50,1.72)-3	28.6	0.543	1.31	1.72	1.90	2.98	L	11.4
PL(0.49,2.00)-3	27.9	0.531	1.41	2.00	1.81	2.89	L	11.3
PL(0.34,1.18)-4	37.2	0.344	1.08	1.18	1.56	3.56	L[f]	12.0
PL(0.34,1.37)-4	36.9	0.339	1.15	1.37	1.53	3.53	G[f]	12.8
PL(0.33,1.43)-4	36.2	0.326	1.17	1.43	1.44	3.44	C[f]	12.9
PL(0.59,1.20)-5	31.9	0.589	1.11	1.20	2.29	3.37	G	10.2
PL(0.58,1.23)-5	31.5	0.584	1.12	1.23	2.24	3.32	G	10.3
PL(0.59,1.73)-5	32.1	0.592	1.36	1.73	2.33	3.41	L	11.5
PL(0.59,1.85)-5	31.9	0.589	1.41	1.85	2.29	3.37	L	12.0
PL(0.62,1.30)-6	34.4	0.619	1.16	1.30	2.60	3.68	G	11.0
PL(0.60,1.32)-6	33.1	0.604	1.17	1.32	2.45	3.53	G	10.8
PL(0.61,1.33)-6	33.5	0.609	1.17	1.33	2.49	3.57	G	10.9
PL(0.62,1.39)-6	34.2	0.617	1.21	1.39	2.57	3.65	G	11.1
PL(0.62,1.62)-6	34.3	0.618	1.32	1.62	2.59	3.67	L	11.9
PL(0.63,1.42)-7	35.6	0.632	1.23	1.42	2.75	3.83	C[g]	10.5
PL(0.64,1.42)-7	36.8	0.644	1.23	1.42	2.89	3.97	C[g]	10.3
PL(0.63,1.57)-7	35.6	0.632	1.30	1.57	2.75	3.83	G[g]	11.2
PL(0.64,1.67)-7	36.7	0.643	1.36	1.67	2.88	3.96	G[g]	11.6

[a] Calculated using M_n of each block, densities at room temperature ($\rho_{PEP} = 0.856$ g/mL,[19] $\rho_{PLA} = 1.265$ g/mL[20]), and with respect to a reference volume of 160 Å^3. The volume fraction of the PLA block is thus $f_{PLA} = N_{PLA}/N_{total}$ with $N_{total} = N_{PEP} + N_{PLA}$. [b] PDI determined by size exclusion chromatography with a refractive index detector in THF at 40 °C, relative to polystyrene standards. [c] Molecular weight determined by ^{1}H NMR spectroscopy. [d] Morphology identified by SAXS. Unless otherwise noted, the indicated morphology was observed between 80 °C and the order−disorder temperature when accessible. [e] Domain spacings of series 1, 2, 3, 5, 6, and 7 are given at 80 °C; series 4 is given at 110 °C. [f] Transitions to different morphologies were observed in this series. The indicated morphology was observed at 160 °C. [g] Transitions to different morphologies were observed in this series. The indicated morphology was observed at 130 °C.

distilled H_2O and methanol, and subsequently dried in vacuo at 40−60 °C. PEP−OH ^{1}H NMR ($CDCl_3$, 500 MHz): 3.6 (m, −C**H**$_2$−OH), 1.2 (m, C**H** and C**H**$_2$), 0.8 (b, doublet, C**H**$_3$). PEP−PLA ^{1}H NMR ($CDCl_3$, 500 MHz): 5.6 (m, −C(O)−C**H**(CH_3)−O−), 4.1 (b, −C**H**$_2$−OC(O)), 1.6 (m, −C(O)−CH−(C**H**$_3$)−O−).

Control of PDI of PEP−PLA. A particular series of PEP−PLA diblock copolymers at the same composition were synthesized according to a procedure similar to that described above. The reactions were terminated at different times after the equilibrium conversion (<100%) had been reached. The conversion was determined by ^{1}H NMR spectroscopy comparing the methyl resonances on PEP with backbone resonances in PLA.

Small-Angle X-ray Scattering (SAXS). SAXS measurements were made on 1 mm samples compression molded at 100 °C under 10 000 psi. Measurements were performed on the University of Minnesota Twin Cities Characterization Facility beamline. Cu Kα X-rays ($\lambda = 1.542$ Å) were generated by a Rigaku RU-200BVH rotating anode fitted with a 0.2 × 2 mm^2 microfocus cathode and Franks mirror optics. Temperature control inside the evacuated sample chamber was accomplished with water cooling and electrically heating the brass-block sample holder. Two-dimensional diffraction images were recorded using a Siemens area detector located at the end of a 2.30 or 1.04 m evacuated flight tube and corrected for detector response before analysis. The two-dimensional images were azimuthally integrated and reduced to the one-dimensional form of scattered intensity vs the spatial frequency q. The principal scattering peak was fitted with a Lorenzian function to locate the maximum of the peak to determine q^*. Samples were annealed for 10 min at each temperature before collecting two-dimensional SAXS patterns.

Results

Synthesis of Controlled Polydispersity Diblock Copolymer Materials. Poly(ethylene-*alt*-propylene)-*b*-poly(DL-lactide) (PEP−PLA) was synthesized by the Al-catalyzed ring-opening polymerization of DL-lactide (LA) in the presence of the PEP−OH macroinitiator.[12] Polymerization reactions were carried out at 90 °C for the time required to reach the equilibrium conversion of LA. Equation 1 describes the conversion of monomer (p) as a function of time for an equilibrium polymerization.

$$p(t) = 1 - e^{-k_{app}t} + \frac{e^{\Delta G/RT}}{[LA]_0}(e^{-k_{app}t} - 1) \qquad (1)$$

Because of active site aggregation,[15] the number of reactive chain ends at any given time is uncertain; thus, this expression is presented in terms of an apparent rate constant, $k_{app} = k_p[M^*]$, where $[M^*]$ is the concentration of active chain ends, t is the reaction time, ΔG is the

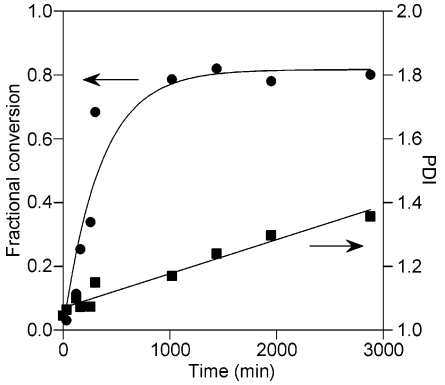

Figure 1. Representative data for the fractional conversion of LA vs time (t) (fit to eq 1) and PDI of the resulting polymer vs time (linear fit as a guide to the eye). Fitting parameters: $k_{app} = (4.76 \pm 1.11) \times 10^{-5}$ s^{-1} and $\Delta G/RT = -1.70 \pm 0.32$ at 90 °C, $[PEP-OH]_0 = 6.4$ mM, and $[Al]_0/[PEP-OH]_0 = 1.0$.

change in Gibbs energy for polymerization, R is the gas constant, and T is temperature. By fitting eq 1 to the measured conversion of LA as a function of time, k_{app} and ΔG may be determined: $k_{app} = (2.06 \pm 1.12) \times 10^{-5}$ s^{-1} and $\Delta G/RT = -2.48 \pm 0.22$ ($[PEP-OH]_0 = 15.0$ mM, $[Al]_0/[PEP-OH]_0 = 0.5$, and 90 °C). These values are consistent with the values determined for the polymerization of LA from hydroxyl-terminated polybutadiene under similar conditions.[15]

Figure 1 shows data for the conversion of LA vs time, with the corresponding fit to eq 1 (fitting parameters: k_{app} and $\Delta G/RT$) and the block copolymer PDI vs time. In the equilibrium polymerization of LA, both polymerization and depolymerization reactions are kinetically significant. Early in the reaction, polymerization dominates the reaction and conversion of LA increases rapidly. As LA is consumed, the rate of polymerization decreases and approaches the rate of depolymerization, which remains essentially constant throughout the course of the reaction. Eventually a dynamic equilibrium is achieved where monomers are randomly added and removed from the active chains. The shuffling of monomers among active chains randomizes chain lengths and broadens the MWD about the same M_n over time. The unimodal broadening of the MWD ceases once the most probable distribution (PDI = 2) has been reached for the PLA block.[16] Therefore, samples allowed to react for different lengths of time after the equilibrium conversion has been reached will possess different MWDs about the same M_n. Assuming formation of each block of a block copolymer are statistically independent events (which they are in this two-step method), the individual block's PDI contributes to the overall diblock copolymer PDI according to eq 2:

$$PDI_{AB} = (PDI_A - 1)w_A^2 + (PDI_B - 1)w_B^2 + 1 \quad (2)$$

where PDI_{AB} is the PDI of the overall diblock copolymer and PDI_A and w_A are the PDI and weight fraction of the A block, respectively.[17] The PDIs of the PEP−OH samples and all diblock copolymers used in this study were obtained by size exclusion chromatography using a refractive index detector (RI-SEC). Although eq 2 was used to estimate the PDI of the PLA block, the chromatogram produced by RI-SEC does not yield the true MWD due to band broadening along the size-exclusion columns during analysis,[18] it allows for self-consistent comparison of the MWDs.

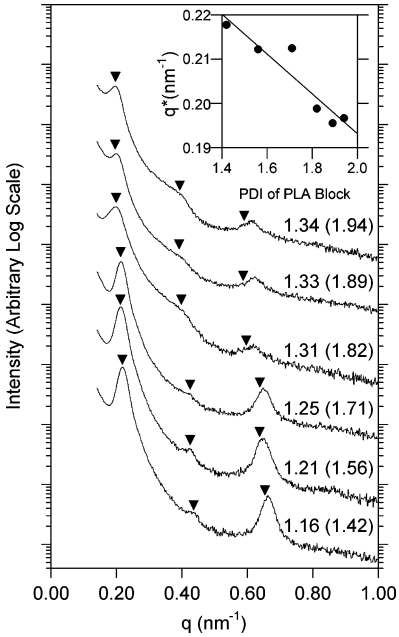

Figure 2. Intensity vs spatial frequency (q) at 80 °C (20 °C above the T_g of the PLA block) for a lamellar structure at strong segregation as PDI is increased for series 1. Overall diblock copolymer PDI is given next to the data, and the PDI of PLA is given in parentheses. Triangles denote q^*, $\sqrt{4}q^*$, and $\sqrt{9}q^*$. The location of q^* was obtained by fitting the primary peak to a Lorenzian function. Inset: q^* (nm^{-1}) vs PDI of PLA.

Morphological Effects of Increased Polydispersity. Table 1 contains the molecular and morphological characteristics of the PEP−PLA diblock copolymers synthesized for this study. Samples are denoted by the volume fraction and PDI of the polydisperse PLA block and the series in which they occur in Table 1; e.g., PL-(0.51,1.42)-1 refers to $f_{PLA} = 0.51$ and $PDI_{PLA} = 1.42$ in the first series in Table 1. The range in composition spans from 0.34 to 0.64 in PLA, and the range in segregation strength ranges from weak ($\chi N \approx 10-20$, series 2−7) to strong segregation ($\chi N \approx 100$, series 1).[12]

Small-angle X-ray scattering (SAXS) was used to determine the morphology of all diblock copolymer materials. Figure 2 shows the SAXS profiles for series 1, symmetric diblock copolymers at strong segregation. All samples in this series exhibited a lamellar morphology. The position of the principal spatial frequency, q^*, decreased as the PDI of the block copolymer increased from 1.16 to 1.34 (see inset, Figure 2). In addition, the scattered intensity (at q^*) noticeably decreased over the same increase in PDI. Equation 3 relates q^* to domain spacing; a decrease in q^* is reflective of an increase in the domain spacing, D.

$$D = \frac{2\pi}{q^*} \quad (3)$$

Table 1 summarizes the domain spacing data for all samples (at 80 °C except where otherwise noted). For all compositions and molecular weights used in this study, an increase in PDI was generally accompanied by an increase in domain spacing; this phenomenon was not limited to systems in the lamellar (L) morphology but also was observed in systems exhibiting the hexagonally packed cylindrical (C) and bicontinuous gyroid (G) morphologies with PDI increasing in both the minority or majority components.

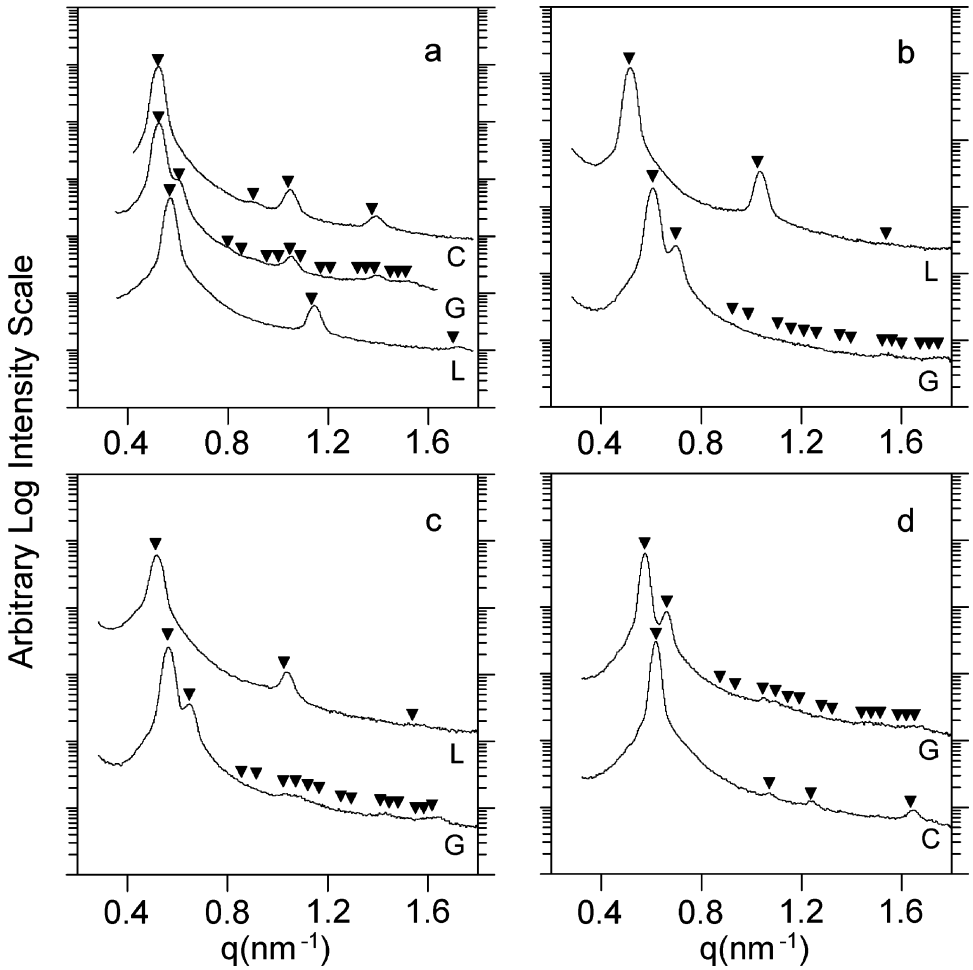

Figure 3. SAXS patterns demonstrating the effects of an increased PDI on the adopted morphology. (▼) Expected peak positions for morphologies indicated. (a) From bottom to top: PL(0.34,1.17)-4, PL(0.34,1.38)-4, and PL(0.33,1.43)-4 at 160 °C. (b) PL(0.59,1.20)-5, PL(0.59,1.85)-5, at 130 °C. (c) PL(0.62,1.30)-6, PL(0.62,1.62)-6 at 130 °C. (d) PL(0.63,1.42)-7, PL(0.63,1.57)-7, at 130 °C.

In addition to increasing domain spacing, an increased PDI led to morphological transitions at constant composition in series 4−7 at intermediate degrees of segregation. PEP−PLA materials with nearly identical compositions possessing the same M_n and at the same temperature possessed different morphologies at different PDIs. Different trends were observed if the PDI was increased in the minority component ($f_{PLA} < 0.5$) vs the majority component ($f_{PLA} > 0.5$). Figure 3 shows the SAXS profiles for several sets of PEP−PLA diblock copolymers that differ significantly only in their PDIs. Series four is presented in Figure 3a at 160 °C. For PL(0.34,1.18)-4, the lamellar morphology was observed. Upon a small PDI increase, PL(0.34,1.37)-4 adopted the gyroid morphology. Increasing the PDI further, PL(0.33,1.43)-4 resulted in the hexagonally packed cylindrical morphology. Figure 3b shows representative scattering patterns at 130 °C from series five. PL(0.59,1.20)-5 was in the gyroid morphology at all temperatures investigated and remained so until disordering. However, PL(0.59,1.85)-5 exhibited peaks indicative of a lamellar structure until disordering. Figure 3c shows representative scattering patterns from series 6 at 130 °C. PL(0.62,1.30)-6 was in the gyroid state, and PL(0.62,1.62)-6, at nearly identical composition but higher PDI, was lamellar. PL(0.63,1.42)-7 and PL(0.63,1.57)-7 also exhibited different ordered states at 130 °C (Figure 3d), hexagonally packed cylinders and gyroid, respectively.

Discussion

Increasing PDI of the PLA block in PEP−PLA block copolymers has been shown to influence the domain spacing and the resultant morphology of these materials. The increase in domain spacing was expected on the basis of mean-field theory predictions[3−6,9] and previous experiments based on multicomponent diblock copolymer blends.[10] The plot in Figure 4 shows the relative experimental lamellar domain spacing as a function of PDI for series 1−3 from Table 1 where the experimental lamellar domain spacing (D) has been normalized by the mean-field theory calculated lamellar domain spacing at PDI = 1 (D_0), to account for the slight compositional differences that exist within each series of samples. For series 1, the strong-stretching theory expression for the lamellar domain spacing (D_{SST}) was used.[21,22]

$$D_{SST} = 1.10 b \chi^{1/6} N^{2/3} \quad (4)$$

An expression for χ was obtained previously by synthesizing a series of compositionally symmetric ($f = 0.5$) and narrow molecular weight distribution PEP−PLA diblock copolymers at different molecular weights and recording the order−disorder temperature.[12] Using the general result of mean-field theories that at $f = 0.5$, the order−disorder transition occurs at $\chi N = 10.495$,[2] an estimate for χ of the form $\chi = 445/T - 0.64$ was obtained

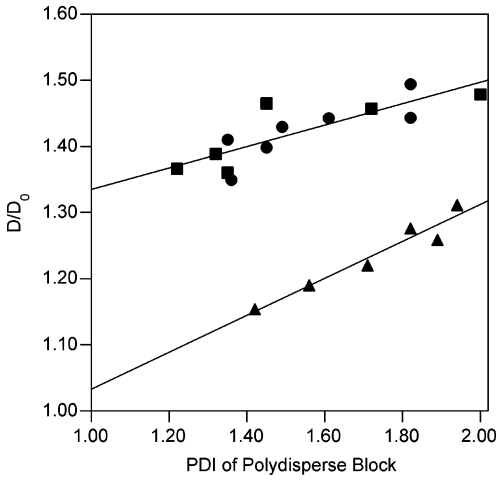

Figure 4. Experimental lamellar domain spacings of series 1 (▲) at strong segregation and series 2 (●) and 3 (■) at intermediate segregation. All domain spacings were measured at 80 °C.

using a reference volume of 174 Å^3.[12] Equation 4 has been directly used by others to determine an estimate for χ.[23,24] However, as seen in Figure 4, the domain spacing is also dependent on the system PDI, which if not accounted for can introduce a significant systematic error into the estimate of χ (e.g., a 30% increase in D leads to an overestimation of χ by a factor of 4.8).

The data for series 1 show an increase in domain spacing with increasing PDI. The intercept of a best-fit line to the data nearly intersects $D/D_0 = 1$ at PDI = 1 at these higher degrees of segregation. For series 2 and 3, a one-dimensional SCMFT was used to calculate the lamellar domain spacing for a perfectly monodisperse system ($D_{MFT(MONO)}$) at the estimated degree of segregation ($\chi N = 25$) and at the composition of the diblock copolymer in question (typically $D_{MFT(MONO)} \approx 4.2R_g$, where R_g is the unperturbed radius of gyration).[25] According to the data in Figure 4, the diblock copolymers in series 2 and 3 are in more extended configurations than predicted by monodisperse SCMFT given that the data do not intercept $D/D_0 = 1$ at PDI = 1 but rather show systematically larger values of D/D_0.

In a related study, Koneripalli et al. blended non-lamellar-forming diblock copolymers such that the average composition ($f_A \approx 0.5$) of the blend led to a lamellar structure and found that the domain spacing of the blend was 5.8% greater than that of a nonblended sample at equivalent average molecular weight and composition.[26] By neutron reflectivity measurements and SCMFT calculations these authors showed that a blended block copolymer melt of short and long chains could more efficiently fill space by using a large chain to fill the center of the microphase-separated domain; the decreased entropic penalty of stretching allows the domain to stretch further to minimize unfavorable segment−segment contacts at the interface. This is consistent with the arguments presented by Milner et al.[5] and should also be true for the case of a polydisperse melt, which may also fill space more efficiently by using large chains to fill the center of the microphase-separated domain.

Koneripalli et al. also demonstrated that SCMFT for these binary diblock copolymer blends underestimated the increase in lamellar domain spacing compared to a monodisperse melt (at equivalent composition). This underestimation was more pronounced as χ was increased in the calculation.[26] Figure 4 reveals that the relative increase in domain spacing as PDI is increased is insensitive to changes in segregation (i.e., the slope of D/D_0 vs PDI data is nearly identical at the two different segregation strengths shown in Figure 4). We have calculated the theoretical relative change in domain spacing as PDI is increased in one block using SCMFT ($D_{MFT(POLY)}/D_{MFT(MONO)}$) and found that the relative increase in domain spacing is dependent on the degree of segregation. For example, at $f_A = 0.5$, $PDI_A = 1$ and $PDI_B = 2$, at $\chi N = 12$ yields $D_{MFT(POLY)}/D_{MFT(MONO)} = 1.46$, at $\chi N = 25$, $D_{MFT(POLY)}/D_{MFT(MONO)} = 1.15$, and at $\chi N = 50$, $D_{MFT(POLY)}/D_{MFT(MONO)} = 1.08$. These data suggest that as χN approaches the strong segregation limit ($\chi N \approx 100$), the SCMFT-calculated domain spacings for monodisperse and polydisperse systems converge to the same value (i.e., in the strong segregation regime, there is predicted to be a negligible increase in domain spacing as PDI is increased for one block). This is in apparent disagreement with the results of this study. The strongly segregated samples appear slightly more sensitive to changes in PDI.

Inspection of one-dimensional density distributions using SCMFT[27] of polydisperse diblock chains reveals that highly asymmetric chains with short B blocks (the polydisperse segment) are actually distributed within the opposing A domains. The small number of B repeating units is not enough to anchor the block copolymer at the A/B interface. This would be seen as a uniform decrease in the small-angle X-ray scattering intensity as the number of smaller chains pulled into the opposing domain increases. In the case of the most probable MWD for PLA, the chains possessing only a few monomer units are numerous. Inspection of the scattering profiles in Figure 2 demonstrates that the scattered intensity decreases as PDI is increased, and we attribute this to mixing of short chains of one component into the opposing domain. The mixing of small B segments into the A-rich domain would also have the effect of swelling that domain.

In addition to domain spacing differences, the ordered state symmetry adopted by the diblock copolymers was also shown to be dependent on the polydispersity in compositionally asymmetric samples in accord with what was observed theoretically by Sides and Fredrickson.[9] The PDI was increased asymmetrically in this work; i.e., the PDI of only one block was increased while that of the other was held fixed. Increasing PDI in the minority block ($f_{PLA} < 0.5$) can cause transitions to morphologies with increased mean interfacial curvature (e.g., L → G → C), whereas increasing PDI in the majority block ($f_{PLA} > 0.5$) leads to morphologies with decreased mean interfacial curvature (e.g., C → G → L). Interfacial curvature for block copolymer melts results from the imbalance of stretching energy between opposing blocks; the curving of the interface alleviates the imbalance by curving the interface toward the component with the lower stretching energy, requiring it to stretch and allowing the component with the larger stretching energy to relax.[28]

As the PDI is increased for one component, the change in morphologies observed in this study is consistent with the stretching energy of that component being reduced, thus favoring morphological transitions to structures with increased interfacial curvature toward the polydisperse component as they stretch further from the interface to maintain the balance of stretching energies

between blocks. As an example of how increased PDI can decrease the stretching energy of a block, consider blocks on the inside of interfacial curvature. These chains are required to stretch to fill the center of the domain. By utilizing large chains present in polydisperse melts to fill this space, unfavorable stretching to fill space uniformly may be avoided. Thus, decreasing the stretching energy of the block and favoring polydisperse chains on the inside of increasing interfacial curvature.

In the polydisperse melt, the mixing of chains with small B segments into the monodisperse A-rich domain can swell the monodisperse domain.[27] If the monodisperse domain is on the outside of interfacial curvature, this can further drive the system toward structures with increased interfacial curvature toward the minority component as the majority domain is swollen. The addition of chains to the majority domain, which are not constrained to the interface, may also relieve packing frustration in nonlamellar morphologies relative to monodisperse systems. On the other hand, if the monodisperse domain is the minority domain (and PDI is increased in the majority domain), the addition of free chains may aid in the stabilization of morphologies with less interfacial curvature toward the minority domain; however, it may destabilize the system relative to macrophase separation in an analogous manner to adding pure homopolymer to the minority domain of a diblock copolymer.[29]

Conformational asymmetry directly affects the balance of stretching energy between block copolymer components as well. We expect that as PDI is increased, the entire phase diagram will change in a manner consistent with increases in conformational asymmetry.[30] That is, increasing polydispersity in one block leads to morphological changes that would be expected by increasing the statistical segment length of that block. Both result in a decrease in stretching energy and thus prompt transitions to morphologies with increased interfacial curvature when increased in the minority domain and to morphologies with decreased interfacial curvature when increased in the majority domain.

Conclusion

Increasing polydispersity has a significant effect on the microphase separation of block copolymers. The domain spacing was found to generally increase at all compositions investigated as PDI was increased in one block of a diblock copolymer while the PDI of the other block remained constant (and small). In addition, the morphology was also dependent on the PDI. Different morphologies were observed at equivalent molecular weight and composition but different polydispersity indices. When the PDI was increased in the minority domain of an asymmetrical diblock copolymer, changes in morphology led to structures with higher mean interfacial curvature. Increasing PDI in the majority domain of an asymmetrical diblock copolymer led to structures with lower mean interfacial curvature. This is consistent with an increased PDI decreasing the stretching energy of the polydisperse block.

Acknowledgment. This work was supported primarily by the MRSEC Program of the National Science Foundation under Award DMR-0212302. The authors thank the Minnesota Supercomputing Institute for computational resources and technical assistance with SCMFT. We also thank Frank S. Bates, Glenn H. Fredrickson, David C. Morse, Scott W. Sides, Amit Ranjan, and Mahesh K. Mahanthappa for helpful discussions.

Supporting Information Available: Description of SCMFT and numerical methods used along with RI-SEC traces of PEP−OH precursor and PEP−PLA diblock copolymers. This material is available free of charge via the Internet at http://pubs.acs.org.

References and Notes

(1) Bates, F. S.; Frederickson, G. H. *Phys. Today* **1999**, *32*.
(2) Leibler, L. *Macromolecules* **1980**, *13*, 1602.
(3) Leibler, L.; Benoit, H. *Polymer* **1981**, *22*, 195.
(4) Hong, K. M.; Noolandi, J. *Polym. Commun.* **1984**, *25*, 265.
(5) Milner, S. T.; Witten, T. A.; Cates, M. E. *Macromolecules* **1989**, *22*, 853.
(6) Burger, C.; Ruland, W.; Semenov, A. N. *Macromolecules* **1990**, *23*, 3339.
(7) Burger, C.; Ruland, W.; Semenov, A. N. *Macromolecules* **1991**, *24*, 816.
(8) Fredrickson, G. H.; Helfand, E. *J. Chem. Phys.* **1987**, *87*, 697.
(9) Sides, S. W.; Frederickson, G. H. *J. Chem. Phys.* **2004**, *121*, 4974.
(10) Matsushita, Y.; Noro, A.; Iinuma, M.; Suzuki, J.; Ohtani, H.; Takano, A. *Macromolecules* **2003**, *36*, 8074. A further contribution was made by forming two- and three-component blends containing the same composition but different MWDs about that composition: Noro, A.; Donghyun, C.; Takano, A.; Matsushita, Y. *Macromolecules* **2005**, *38*, 4371.
(11) Bendejacq, D.; Ponsinet, V.; Joanicot, M.; Loo, Y.-L.; Register, R. A. *Macromolecules* **2002**, *35*, 6645.
(12) Schmidt, S. C.; Hillmyer, M. A. *J. Polym. Sci., Part B: Polym. Phys.* **2002**, *40*, 2364.
(13) Anderson, K. S.; Hillmyer, M. A. *Macromolecules* **2004**, *37*, 1857.
(14) Pangborn, A. B.; Giardello, A.; Grubbs, R. H.; Rosen, R. K.; Timmers, F. J. *Organometallics* **1996**, *15*, 1518.
(15) Wang, Y.; Hillmyer, M. A. *Macromolecules* **2000**, *33*, 7395.
(16) Rempp, P.; Merrill, E. W. *Polymer Synthesis*, 2nd ed.; Hüthig & Wepf Verlag: Basel, 1991.
(17) Almdal, K. Recent Developments in Synthesis of Model Block Copolymers Using Ionic Polymerisation. In *Developments in Block Copolymer Science and Technology*; Hamley, I. W., Ed.; John Wiley and Sons: Hoboken, NJ, 2004.
(18) Lee, W.; Lee, H.; Cha, J.; Chank, T.; Hanley, K. J.; Lodge, T. P. *Macromolecules* **2000**, *33*, 5111.
(19) Fetters, L. J.; Lohse, D. J.; Richter, D.; Witten, T. A.; Zirkel, A. *Macromolecules* **1994**, *27*, 4639.
(20) Witzke, D. R.; Narayan, R.; Kolstad, J. T. *Macromolecules* **1997**, *30*, 7075.
(21) Matsen, M. W.; Bates, F. S. *J. Polym. Sci., Part B: Polym. Phys.* **1997**, *35*, 945.
(22) Semenov, A. N. *Sov. Phys. JETP* **1985**, *61*, 733.
(23) Ren, Y.; Lodge, T. P.; Hillmyer, M. A. *Macromolecules* **2002**, *35,* 3889.
(24) Davidock, D. A.; Hillmyer, M. A.; Lodge, T. P. *Macromolecules* **2004**, *37*, 397.
(25) Rasmussen, K. Ø.; Kalosakas, G. *J. Polym. Sci., Part B: Polym. Phys.* **2002**, *40*, 1777.
(26) Koneripalli, N.; Levicky, R.; Bates, F. S.; Matsen, M. W.; Anker, J.; Kaiser, H. *Macromolecules* **1998**, *31*, 3498.
(27) See ref 9, Figure 3. The first term in their Gauss−Laguerre quadrature ($g = 1$) of the density distribution of B monomers corresponds to the chains of shorter length in the polydisperse block. It is evident from their figure that the density of these chains possessing the shortest chains of the polydisperse component are present in the opposite phase at $\chi N = 18$; i.e., the shortest chains are weakly anchored to the interface and are pulled free into the opposing phase. Inspection of Figure 5 of ref 9 demonstrates the swelling of both the monodisperse and polydisperse phases as PDI is increased in the hexagonally packed cylindrical morphology. This spreading of B monomers throughout a microphase-separated AB diblock copolymer melt would produce a decrease in scattered intensity since the electron density contrast between the phases would be reduced. Calculations done in the course of this study using the Sides and Fredrickson methodology have

demonstrated this to occur in lamellar systems as well. It should be noted however that as expected, as segregation increases, the infiltration of one domain by even short segments of the other component occurs increasingly less.
(28) Matsen, M. W.; Bates, F. S. *Macromolecules* **1996**, *29*, 7641.
(29) Matsen, M. W. *Macromolecules* **1995**, *28*, 5765.
(30) For an excellent discussion on how a change in the stretching energy of one component can change both the domain spacing and resultant morphology see: Matsen, M. W.; Thompson, R. B. *J. Chem. Phys.* **1999**, *111*, 7139.

MA051025R